Journal of Nuclear Materials 412 (2011) 321–326

Contents lists available at ScienceDirect

Journal of Nuclear Materials

journal homepage: www.elsevier.com/locate/jnucmat

# In situ transmission electron microscopy of electron-beam induced damage process in nuclear grade graphite

C. Karthik [a,b,*], J. Kane [a,b], D.P. Butt [a,b], W.E. Windes [b,c], R. Ubic [a,b]

[a] Department of Materials Science and Engineering, Boise State University, 1910 University drive, Boise, ID 83725, United States
[b] Centre for Advanced Energy Studies, 995 University blvd, Idaho Falls, ID 83415, United States
[c] Idaho National Laboratory, 2351 N. Boulevard, Idaho Falls, ID 83415, United States

ARTICLE INFO

*Article history:*
Received 15 December 2010
Accepted 19 March 2011
Available online 29 March 2011

ABSTRACT

Atomic level processes involved in the swelling and crack-closing in nuclear grade graphite under electron irradiation have been observed in real-time using transmission electron microscopy. Noise-filtered lattice images show the formation of vacancy loops, interstitial loops and resulting dislocations with unprecedented clarity. The dislocation dipoles formed via vacancy loops were found to undergo climb resulting in extra basal planes. Concurrent EELS studies showed a reduction in the atomic density because of the breakage of hexagonal carbon rings. The formation of new basal planes via dislocation climb in addition to the bending/breaking of basal planes leads to swelling and closing of micro-cracks.



## 1. Introduction

Artificial polycrystalline nuclear graphite will be used as a major structural and moderator material in high-temperature gas-cooled next-generation nuclear reactors [1]. Nuclear graphite has a complex microstructure consisting of filler particles, binder and micro-cracks parallel to the basal planes [2–4]. Since the historic nuclear graphite grades are no longer available, it is necessary to develop an understanding of irradiation induced dimensional and property changes in the current and future grades. For this reason, there has recently been renewed interest in the characterization of the properties of nuclear graphite [5–10].

Under irradiation, polycrystalline graphite undergoes complex dimensional changes, whereas single-crystalline graphite such as highly oriented pyrolytic graphite (HOPG) undergoes elongation in a direction perpendicular to the basal planes and shrinkage along the basal planes [2]. The present understanding is that the displacement of carbon atoms caused by irradiation results in the accumulation of interstitial loops in-between the basal planes forcing them apart. These interstitial clusters eventually rearrange to form into new basal planes resulting in the expansion along *c*-axis and the *a*-axis contraction is explained at present by the formation of vacancy loops. At present it is argued that the bulk changes in polycrystalline graphite can be explained by the orientation of the crystallites coupled with accommodation provided by micro-cracks oriented parallel to the basal planes [8]. The micro-cracks accommodate the *c*-axis expansion resulting in net shrinkage at lower doses of irradiation [11–13] provided by the *a*-axis shrinkage. However, this explanation was disputed by Tanabe et al. [14,15], whose room temperature electron microscopic studies on carbon fibers did not show any evidence for the formation of interstitial basal planes and their existence at room temperature is controversial to date. Niwase [16,17] proposed a convincing model to explain the dimensional change as well as irradiation induced amorphization at lower temperatures based on the accumulation of partial dislocations, yet the nature of such dislocations remains unknown. The reasons for the lack of clear understanding of radiation induced microstructural changes is the complex microstructure of nuclear graphite as well as the difficulty in capturing the microstructural changes in real-time given the dynamic nature of the process. One of the ways to overcome these difficulties is to use electron-beam (as a substitute for neutrons) in a TEM to simulate the reactor environment which enables real-time observations. However, the dose rates of electron irradiation ($\sim 10^{-4}$ to $10^{-3}$ dpa/s) is much higher than neutron irradiation ($\sim 10^{-7}$ dpa/s). Furthermore, unlike electrons, neutrons and ions produce cascade damage owing to their heavier mass. Nevertheless, the microscopic studies have shown the neutron-induced damage in graphite to be similar to that of electrons which is believed to be because of the large open space between the basal planes [18,19]. The openness of graphite results in less dense neutron-induced cascade structures compared to other close-packed materials which combined with the lower neutron dose rates in usual reactor environments result in annealing of cascade structures leaving a small number of point defects between cascades. Koike and Pedraza [20,21] have carried out detailed microscopic studies on HOPG as well as nuclear graphite and established the

* Corresponding author at: Department of Materials Science and Engineering, Boise State University, 1910 University drive, Boise, ID 83725, United States. Tel.: +1 208 426 5136; fax: +1 208 426 2470.
*E-mail address:* karthikchinnathambi@boisestate.edu (C. Karthik).

0022-3115/$ - see front matter © 2011 Elsevier B.V. All rights reserved.
doi:10.1016/j.jnucmat.2011.03.024

similarities between electron and neutron-induced damage processes. However, as pointed out by Pedraza [21] one should not directly compare the calculated dpa values because of the difference in the dose rates and the consequent difference in the rate of defect pairs generated.

In the present study, the room temperature electron irradiation induced swelling, crack-closing, and associated microstructural processes performed on next-generation nuclear-grade graphite (grade NBG-18) were observed in situ using a transmission electron microscope (TEM). The changes in the local lattice structure of nuclear grade graphite under electron irradiation, especially the evidence for the formation of interstitial loops have been shown with unprecedented clarity with the aid of noise-filtered high resolution electron microscopic (HREM) images obtained from videos recorded in situ. EELS was also been used to monitor the changes in the bonding environment as well as the atomic density of the graphite.

## 2. Experimental

TEM samples of commercial nuclear-grade graphite, NBG-18 (supplied by SGL group, Germany), were prepared by conventional sample preparation techniques. Disks with 3 mm diameters were cut from the as-received bulk graphite. These disks were further thinned mechanically to approximately 100 μm thick. An ion-slicer (EM09100-IS, JEOL) was used to achieve the final electron transparency. Compared to conventional ion milling techniques, the ion-slicer is known to produce minimal beam damage to the samples. In situ electron irradiation and EELS studies were performed at room temperature on a 200 kV JEOL-2100 high resolution transmission electron microscope fitted with an EELS spectrometer (Enfina, Gatan). Since the irradiation induced processes were rapid, the whole process was captured in the form of a video. The noise reduction of the videos was carried out via notch-pass filtering of fast Fourier transforms. The entire filtering process was carried out using a MATLAB® code developed at Boise State University.

## 3. Results and discussion

Fig. 1a and b show the microstructure of NBG-18 taken from filler and binder regions respectively. The complex microstructure of nuclear graphite arises from the manufacturing process which involves mixing coke filler particles (petroleum or coal tar) with a binder (pitch). The micro-cracks seen in Fig. 1a are formed due to the anisotropic crystal thermal expansion coefficient leading to de-lamination when the graphite billets cool from high graphitization temperatures. These micro-cracks play a vital role in determining the magnitude of irradiation induced swelling as they can accommodate crystalline swelling that occurs at lower irradiation doses. Fig 1b shows a region of binder which is embedded with rosette like particles which are resultant of graphitization of solid quinoline insoluble particles made up of high molecular weight aromatic molecules present in the pitch binder [4].

The electron irradiation induced microstructural changes, in particular the closing of micro-cracks were studied in the filler particles where they are long and lenticular in nature and are believed to have the most influence on irradiation induced property changes. Fig 2 shows the effect of intense electron irradiation on the micro-cracks. The electron-beam was focused ($\sim 5 \times 10^{21}$ electrons/cm-s) and positioned to cover the center of the micro-crack with an initial width at the center of about ~20 nm. With increased irradiation, the graphite showed significant swelling and the crack closed completely after only 20 s irradiation time. The dosage, in terms of displacement per atom (dpa) was estimated to be approximately 1 dpa. A significant decrease in the diffraction contrast in the irradiated area as seen from Fig. 2b indicates a decrease in the crystallinity in the graphite. Such behavior has been reported elsewhere [7].

Fig 3a–c shows lattice images recorded along [1 0 0 0] depicting the sequential changes in the (0 0 0 2) basal planes associated with swelling and crack-closing induced by electron irradiation. The crack with a width which was ~20 nm seen in Fig. 3a completely disappeared as seen in Fig. 3c due to swelling of the crystallite from either sides. It is clearly shown that, with the increased electron dose, the graphite basal planes lose their long-range order with the formation of breaks and bends, eventually leading to randomization. The shape of the (0 0 0 2) reflections in the corresponding Fast Fourier Transformation (FFT) patterns transformed from spots to arcs (Fig. 4), which is an indication of fragmentation and rotation of the basal planes while still retaining a layered structure locally within a smaller scale of few nanometers as seen from the micrographs. The average (0 0 0 2) inter-planar spacing was estimated to increase approximately 13% from 3.6 nm to 4.2 nm.

During the initial stages of electron irradiation, the nucleation of numerous dislocation dipoles was observed, the concentration of which increased with increasing dpa. A high-magnification lattice image shown in Fig. 3d depicts few of these dislocation dipoles (marked with arrows). These dislocations were created by the formation of vacancy loops (Fig. 3a inset). These images are highly noisy due to the fast scan rate used to capture the rapid changes in the lattice structure. In order to observe these changes more clearly Fig. 5a shows a noise-filtered HREM image, this clearly shows the nucleation of a vacancy loop (marked with arrows) which leads to the formation of a set of edge dislocations with opposite Burgers vectors as shown in Fig. 5b. These two snapshots

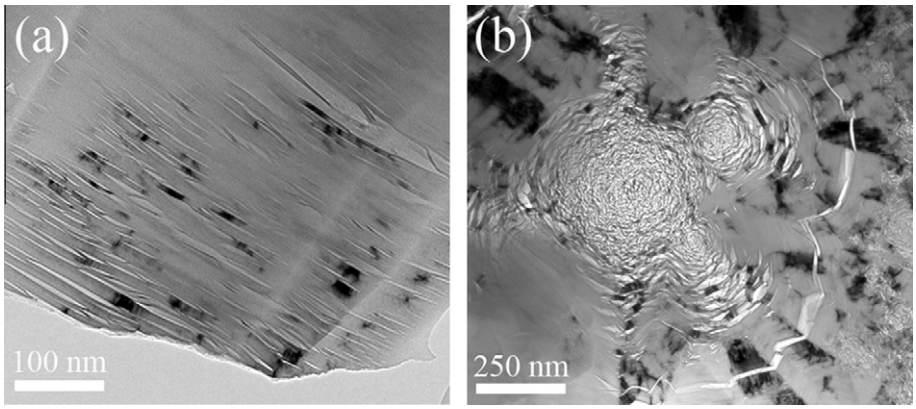


**Fig. 1.** Bright field TEM micrographs showing the microstructure of NBG-18 grade nuclear graphite recorded from (a) filler and (b) binder region.

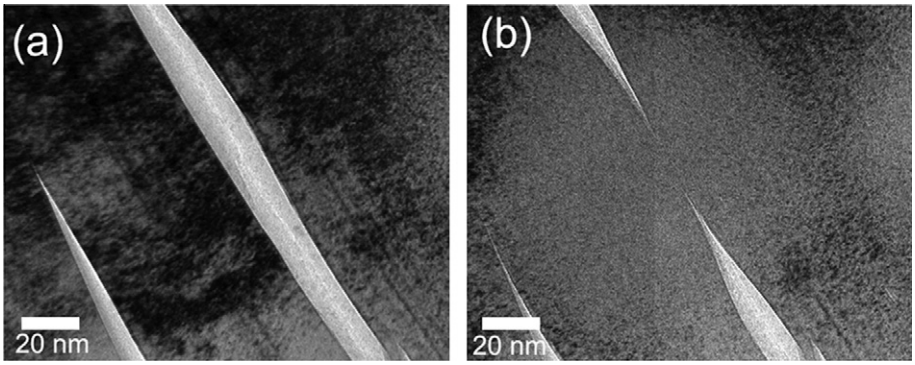


**Fig. 2.** Bright field TEM micrographs showing the effect of electron irradiation on nuclear graphite; (a) shows a micro-crack present in the as-prepared sample and (b) the same crack after ~1 dpa irradiation.

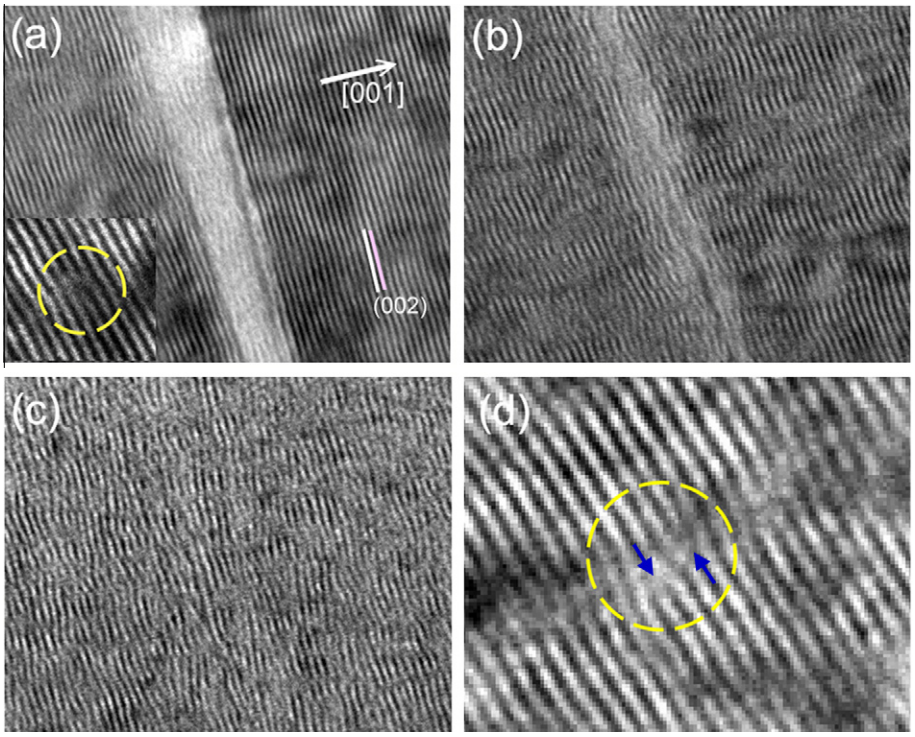


**Fig. 3.** High resolution TEM images showing the effect of electron irradiation on the graphite lattice. (a)–(c) Recorded sequentially from as-prepared, ~0.5 dpa and ~1 dpa irradiated samples. Inset in (a) shows the nucleation of vacancy loops. (d) Close up view of the lattice recorded after ~0.25 dpa showing the creation of dislocation dipoles; one such marked with a dashed circle.

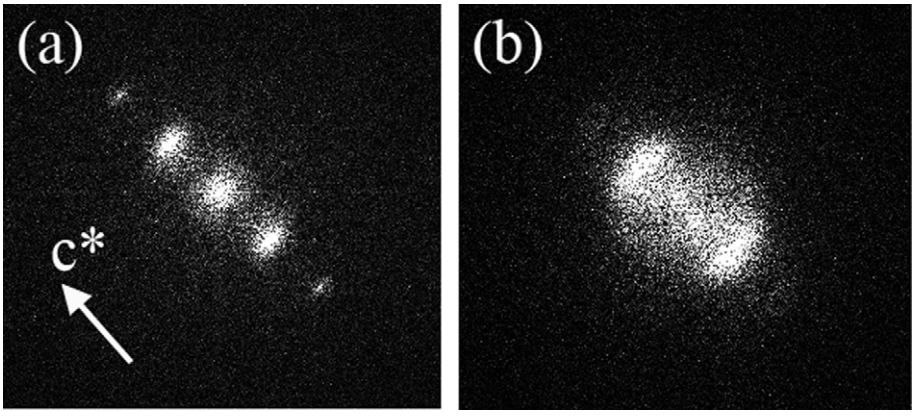


**Fig. 4.** Fast Fourier Transformation (FFT) of HREM images recorded from (a) as-prepared and (b) ~1 dpa irradiated sample.

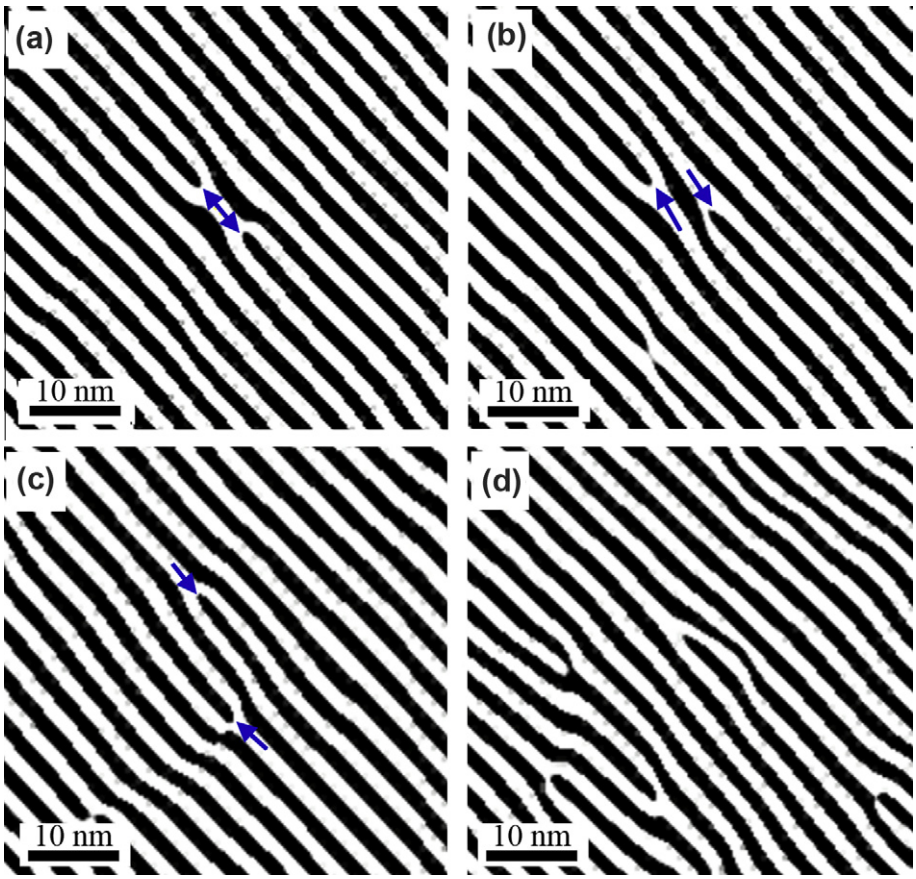


**Fig. 5.** Noise filtered HREM images showing the formation of dislocation dipoles via vacancy loops (a) shows the nucleation of a vacancy loop (~0.25 dpa) dissociating itself into a set of dislocations as shown in (b) with the incomplete planes marked with arrows, (c) shows the growth of the incomplete planes via positive climb and (d) shows the accumulation of several dislocations at higher irradiation doses resulting in disordering of the graphite lattice. Distance between two black fringes corresponds to (0 0 0 2) inter-planar spacing (~0.36 nm).

were captured at 1 s interval. Fig 5b also shows the nucleation of more vacancy loops. It should be noted that the ballistic displacement of carbon atoms under intense electron irradiation results in high concentration of vacancies and interstitials. According to Amelinckx [22], these dislocation loops, formed due to the precipitation of vacancies are known to contain a low-energy single stacking fault (one layer of rhombohedral stacking) with a Burgers vector of $(1/2)\langle 0\,0\,0\,1\rangle + (1/3)\langle -1\,2\,1\,0\rangle$. Subsequent snapshots show that these dislocations move via positive climb as illustrated in Fig. 5c. Fig 5c clearly shows the growth of the incomplete planes marked with arrows which effectively results in the formation of an extra basal plane. In the case of neutron irradiation, it has been assumed from TEM observations of irradiated graphite [23] that the formation of interstitial loops is the reason for the swelling along *c*-axis, but the images presented here for electron irradiation show that extra basal planes can form without the initial formation of interstitial loops. It should be noted that the whole process is dynamic with numerous dislocations being constantly created and annihilated with only a few dislocations undergoing climb. Apart from vacancy loops, the formation of interstitial loops (precipitation of interstitials) was also observed as shown in Fig. 6a and b. Fig. 6a shows the bending of planes outward indicative of compressive stress exerted by interstitial cluster even though the loop is not resolvable by the Fourier analysis. According to Muto and Tanabe [15], the interstitial loops would require to be larger than half the sample thickness to be visible in HREM images. Fig 6b, a subsequent snap shot recorded after 1 s irradiation shows a more fully grown interstitial loop with a lateral length of about ~5 nm. Most of the loops observed in this work were of similar size. The interstitial loops of sufficient size are considered to introduce a new *c* layer in the *ab* stacking of hexagonal graphite. This type of interstitial loops, also referred to as prismatic dislocation loops are essentially partial dislocations with a Burgers vector of ½[0 0 0 1] [24]. These interstitial loops were found to be highly unstable and destroyed by further electron irradiation. With the increased irradiation, the concentration of dislocations also increased, leading to an increase in the concentration of broken graphite layers, eventually leading to more randomization as shown in Fig. 5d. The complete real-time noise-filtered video of the above mentioned processes is provided in video 1.

In order to obtain a better understanding of the implications of the electron irradiation damage on the atomic bonding, EELS was used to study the changes in the bonding environment associated with breakage and randomization of the graphite layers. Fig. 7 shows the low-loss and core-loss EELS spectra recorded for as-prepared and after 1 dpa irradiation corresponding to the microstructures shown in Fig. 3a and c. The low-loss spectrum shown in Fig. 7a has two prominent features, a $\pi$-plasmon peak around 6 eV and $\pi + \sigma$ plasmon peak around 25 eV. The $\pi + \sigma$ plasmon peak showed a shift towards lower energies with an increase in the irradiation damage. The energy shift was 1.9 eV for 1 dpa irradiation. A shift towards lower energies indicates a reduction in valance electron density which could be indicative of a volume expansion or of structural transitions such as the formation of non-six sided carbon rings [25]. It should be noted that there is a weak $\pi$-plasmon peak still present even after 1 dpa irradiation

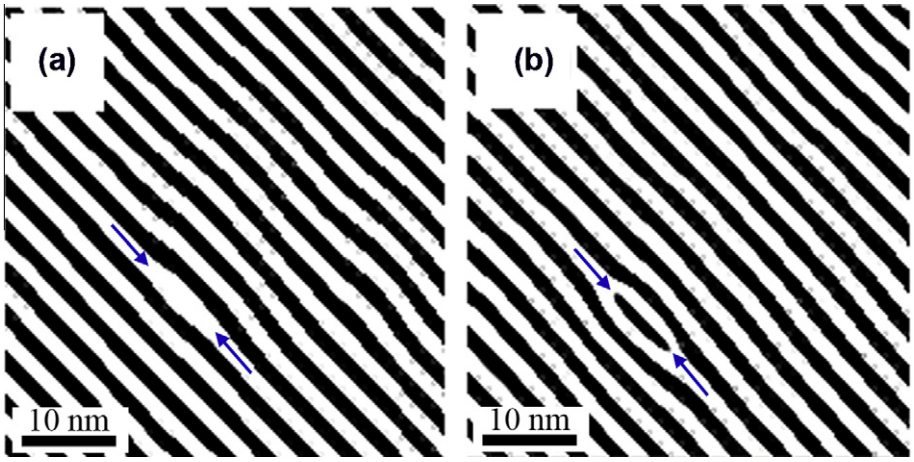


**Fig. 6.** (a) Nucleation and (b) growth of an interstitial loop.

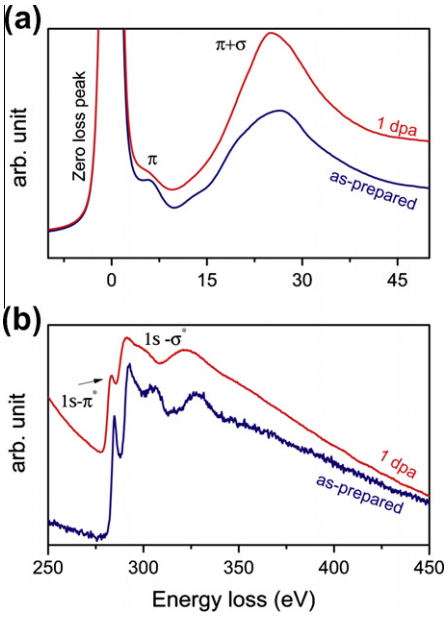


**Fig. 7.** (a) Low-loss and (b) core-loss EELS spectra of the graphite recorded from the as-prepared and ~1 dpa irradiated graphite.

indicating that the layered structure associated with π-bonds is retained, although largely aperiodic, even at this stage of irradiation, confirming the microstructural observations of the present study.

From the peak position ($E_p$) of the π + σ plasmon peak, the change in the valence electron density ($n_e$) of the graphite was calculated using a relationship based on the quasi-free electron model [26],

$$E_p = \hbar \frac{n_e e^2}{\varepsilon_0 m^*} \tag{1}$$

where $m^*$ is the effective mass of electrons (for graphite, $m^* = 0.87 m_e$, where $m_e$ is the free electron mass [27]) and $\varepsilon_0$ is the permittivity of free space. The mass density can then be estimated from $n_e$ using the atomic mass of carbon and the number of valance electrons per carbon (4). This method of calculating mass density has been used and verified by several authors [27,28]. From Fig. 7a, the densities of the as-prepared and ~1 dpa irradiated graphite have been estimated to be 2.28 g/cm$^3$ and 1.96 g/cm$^3$, respectively; an average fall in density drop of about 16%. It should be noted that the density of the as-prepared graphite is essentially the theoretical density of single-crystalline graphite (2.26 g/cm$^3$), which gives validation to this method.

The *K*-edge core-loss spectra for the corresponding doses are shown in Fig. 7b. The spectra have two main features: a peak at ~285 eV and a maximum with extended fine structures at ~ 290 eV which are attributed to 1s-π* and 1s-σ* electronic transitions, respectively. It can be seen that the fine structure in the σ* peak disappeared with the formation of a broad peak, which is indicative of the formation of fullerene like structures [29]. This change indicates the deterioration of the long-range periodicity within the basal plane due to the formation of non-hexagonal atomic rings, which corroborates the previously calculated reduction in density. Apart from destroying the long range ordering, the dislocation dipoles are also believed to aid the formation of the so-called bucky onions [17] because the dipoles induce curvature of the basal planes which is consistent with the formation of bends and curves in the present case and may explain the changes observed in the EELS spectra. Recently, Chuvlin et al. [30] have shown in real-time the fullerene formation from a graphene sheet under electron irradiation. Also, the accumulation of interstitial carbon atoms themselves can induce, local buckling of basal planes by forming cross-links between the basal planes.

Initially, the formation and growth of new interstitial planes as a result of accumulation of displaced carbon atoms were considered to be the sole reason for the macroscopic swelling of graphite along the *c*-axis, but there was no clear microstructural evidence creating doubt as to the above mentioned hypothesis for *c*-axis expansion [24]. In this work, clear evidence for the formation of interstitial loops at room temperature has been shown. However, the interstitial loops were found to be highly unstable and few in number, therefore unlikely to significantly contribute to the observed swelling. Hence, the authors believe that the observed swelling along *c*-axis and the closing of micro-cracks is mainly because of the new basal planes being introduced by the positive climb of dislocation dipoles created via vacancy loops. The dislocation climb involves the migration and effective accumulation of carbon atoms along *c*-axis leaving behind a high concentration of vacancies, the condensation of which on free surfaces might be a reason for the *a*-axis shrinkage. In addition, the significant reduction in density observed even at 1 dpa of electron irradiation shows the increase in the open nature of the lattice. As proposed by Niwase [16], as the dislocation dipoles increase in concentration, they introduce breaks, bends and curls in the basal planes, leading to the destruction of the lattice ordering and resulting in a more open structure which is confirmed from the increase in the measured lattice parameter and decrease in density as shown by EELS study.

## 4. Conclusions

The in situ HRTEM study and analysis of electron irradiation damage in graphite presented in this paper provides experimental evidence for the formation of vacancy loops and interstitial loops in graphite irradiated at room temperature. Dislocations were found to undergo positive climb resulting in the formation of extra basal planes which in addition to the reduction in atomic density as evidenced by EELS are believed to be responsible for the observed swelling and crack-closure.

## Acknowledgements

This material is based upon work supported by the Department of Energy [National Nuclear Security Administration] under Award Numbers 00041394/00026 and DE-NE0000140. TEM studies were carried out at the Boise State Centre for Materials Characterization (BSCMC) and were supported by NSF MRI Grant DMR-0521315. Furthermore, J. Kane acknowledges the funding of the Nuclear Regulatory Commission under the Nuclear Materials Fellowship Program (NRC-38-08-955).

## Appendix A. Supplementary materials

Supplementary data associated with this article can be found, in the online version, at doi:10.1016/j.jnucmat.2011.03.024.

## References

[1] T.R. Allen, K. Sridharan, L. Tan, W.E. Windes, J.I. Cole, D.C. Crawford, G.S. Was, Nucl. Technol. 162 (2008) 342.
[2] R.E. Nightingale, Nuclear Graphite, Academic press, New York, 1962.
[3] A.N. Jones, G.N. Hall, M. Joyce, A. Hodgkins, K. Wen, T.J. Marrow, B.J. Marsden, J. Nucl. Mater. 381 (2008) 152.
[4] K.Y. Wen, T.J. Marrow, B.J. Marsden, Carbon 46 (2008) 62.
[5] B.J. Marsden, G.N. Hall, O. Wouters, J.A. Vreeling, J. van der Laan, J. Nucl. Mater. 381 (2008) 62.
[6] L.L. Snead, T.D. Burchell, Y. Katoh, J. Nucl. Mater. 381 (2008) 55.
[7] K.Y. Wen, J. Marrow, B. Marsden, J. Nucl. Mater. 381 (2008) 199.
[8] G. Hall, B.J. Marsden, S.L. Fok, J. Nucl. Mater. 353 (2006) 12.
[9] T.D. Burchell, L.L. Snead, J. Nucl. Mater. 371 (2007) 18.
[10] T.D. Burchell, J. Nucl. Mater. 381 (2008) 46.
[11] W. Bollmann, J. Appl. Phys. 32 (1961) 869.
[12] C. Baker, A. Kelly, Phil. Mag. 11 (1965) 729.
[13] A. Kelly, R. Mayer, Phil. Mag. 19 (1969) 701.
[14] T. Tanabe, S. Muto, K. Niwase, Appl. Phys. Lett. 61 (1992) 1638.
[15] S. Muto, T. Tanabe, Phil. Mag. A 76 (1997) 679–690.
[16] K. Niwase, Phil. Mag. Lett. 82 (2002) 401.
[17] K. Niwase, Mater. Sci. Eng. A 400 (2005) 101.
[18] J.H.W. Simmons, Radiation Damage in Graphite, Pergamon Press, Oxford, 1965.
[19] D.F. Pedraza, Mater. Res. Soc. Symp. Proc. (1992) 437.
[20] J. Koike, D.F. Pedraza, J. Mater. Res. 9 (1994) 1899.
[21] D.F. Pedraza, J. Koike, Carbon 32 (1994) 727.
[22] S. Amelinckx, P. Delavignette, Phys. Rev. Lett. 5 (1960) 50.
[23] P.A. Thrower, W.N. Reynolds, J. Nucl. Mater. 6 (1963) 221.
[24] R.H. Telling, M.I. Heggie, Phil. Mag. 87 (2007) 4797.
[25] M. Takeuchi, S. Muto, T. Tanabe, S. Arai, T. Kuroyanagi, Phil. Mag. A 76 (1997) 691.
[26] R.F. Egerton, Electron Energy-Loss Spectroscopy in the Electron Microscope, Plenum, New York, 1986.
[27] A.C. Ferrari, A. Libassi, B.K. Tanner, V. Stolojan, J. Yuan, L.M. Brown, S.E. Rodil, B. Kleinsorge, J. Robertson, Phys. Rev. B 62 (2000) 11089.
[28] R. Haerle, E. Riedo, A. Pasquarello, A. Baldereschi, Phys. Rev. B 65 (2001) 045101.
[29] M. Takeuchi, S. Muto, T. Tanabe, H. Kurata, K. Hojou, J. Nucl. Mater. 271 (1999) 280.
[30] A. Chuvilin, U. Kaiser, E. Bichoutskaia, N.A. Besley, A.N. Khlobystov, Nature Chem. 2 (2010) 450.